Prototyping a thermal monitoring system for the one-metre aperture Lunar Laser Ranger tube assembly based at the Hartebeesthoek Radio Astronomy Observatory

Poster presented at the 20th International Workshop on Laser Ranging, GFZ Helmholtz Centre, Potsdam, Telegrafenberg - October 9-14, 2016

Philemon Tsele[1], Ludwig Combrinck[2,1], Bongani Ngcobo[1]

[1] Department of Geography, Geoinformatics and Meteorology, University of Pretoria, South Africa

[2] Space Geodesy Programme, Hartebeesthoek Radio Astronomy Observatory, Krugersdorp, South Africa

Abstract

The Hartebeesthoek Radio Astronomy Observatory of South Africa is currently developing a Lunar Laser Ranger (LLR) system in collaboration with National Aeronautics and Space Administration (NASA) and the Observatoire de la Côte d'Azur (OCA). This LLR will add to a limited number of operating LLR stations globally and it is therefore expected to achieve sub-centimetre range precision to the Moon. Key to this expected achievement is the development of a thermal monitoring system for the LLR telescope structure that can account for thermal effects, mainly induced by the telescope's interaction with the varying thermal environment. In particular, we present a prototype of the thermal monitoring system in which resistance temperature detectors (RTD) sensors were used to measure and predict thermal gradients on the tube assembly. The results obtained will be used to complete the development of a temperature monitoring and control system for accurate pointing of the LLR telescope. In order to measure and predict the temperature gradients across the tube surface, two sets of RTD sensors were installed. One set was used to measure temperature and the other set was used to validate the predicted temperature. Temperature regions (without sensors) of the telescope tube were mapped at the RMS that varied between 0.19 and 0.24 °C which confirms the accuracy of the interpolation method. For tube temperature in the range 19-21 °C, the calculated thermal gradients were found to be about 0.5 °C. The larger gradients (>> 1.0 °C) ought to be regulated to minimize their influence on pointing.

1. Introduction

Ground-based telescopes utilized for laser ranging observations of space-based targets can be affected by thermal gradients and related structural deformations, known to be detrimental to the telescope pointing performance [1]. This is more so on the Lunar Laser Ranger (LLR) one-metre aperture telescope that is being constructed at the Hartebeesthoek Radio Astronomy Observatory (HartRAO) in collaboration with NASA and the Observatoire de la Côte d'Azur (OCA) of France. The HartRAO LLR is expected to make ranging observations to the corner cube retroreflectors located on the lunar surface with sub-centimetre level accuracy. Currently, a prototype pointing model operated on a 125 mm dual refractor testbed telescope, placed in a fairly stable environment achieved RMS error values at the 0.5 arcsecond level [2]. Key to the achievement of the required 1 arcsecond pointing accuracy of the HartRAO LLR, is active thermal control measures for providing real-time temperature monitoring and modelling of temperature gradients and related deformations of the telescope structure. Such information could be useful in the pointing model to ensure correction of thermally-induced pointing errors. In particular, the objective of this work was to report on the progress results pertaining the prototype of a thermal monitoring system for the HartRAO LLR tube assembly.

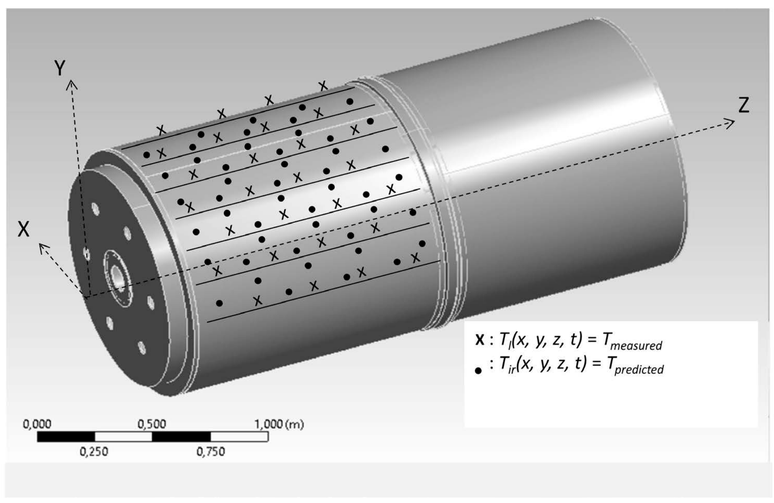

Figure 1: Illustration of the one-metre aperture LLR tube model depicting the even distribution of RTD sensors placed at marked positions ('x'). RTD sensor measurements were used to predict tube temperature at unmeasured locations ('●') where reference sensors are also placed. The back-end of the tube is insulated by the one-metre Zerodur primary mirror that is located at the back of the tube.

2. Thermodynamic properties of the experimental tube

Table 1. show the selected thermal properties of the telescope tube (Figure 1) that were critical parameters for the Finite element (FE) thermal analysis in this study.

Table 1: Thermal properties the aluminium tube.

Specific heat C_p [J/kg.K]	Density p [kg/m^3]	Convection coefficient h [W/m^{2}K]	Thermal Conductivity k [W/m.K]	Coefficient of thermal linear expansion α [K^{-1}]
896-900	2700	5-25	204	23.6 x 10^{-6}

3. Experimental setup

Figure 1 show the Resistant Temperature Detector (RTD) sensors divided into rows along the z-axis where each row can either be of a reference type or of a measured type (T_i (x, z)). The reference sensors were used to compare the effectiveness of the interpolation done to predict the temperature at locations where reference sensors are positioned. In particular, data at the nodal position of each type of the above-mentioned sensors was recorded continually by a data acquisition unit (DAQ), and subsequently used in the finite element (FE) method for tube temperature prediction, calculation of thermal gradients and deformations.

4. Conduction and convective heat transfer

4.1. Conductive boundary conditions

The heat transferred across the cylindrical telescope tube due to conduction is given by:

$$\frac{1}{r}\frac{\partial T}{\partial r}(rk_{rr}\frac{\partial T}{\partial r})-\frac{\partial T}{\partial z}(k_{zz}\frac{\partial T}{\partial r})=Q(r,z) \qquad (1)$$

where r , z are the cylindrical coordinates; k_{rr} and k_{zz} represent the thermal conductivities of the tube along the r and z coordinates, respectively. Q is the heat transferred per unit volume.

4.2. Conduction and convective heat transfer

The heat transferred across the tube due to conduction and convection is given by:

$$\frac{1}{r}\frac{\partial T}{\partial r}(k_{xx}\frac{\partial T}{\partial r})-(k_{zz}\frac{\partial T}{\partial y})+\mathrm{h}_c(T-T_{ambient})=q_n \qquad (2)$$

4.3. Finite element modelling of tube heat transfer

The mathematical description of the FE modelling equation for the cylindrical tube can be found in [4]. In this study, the predicted temperature T_i (at the i^{th} node without a sensor) was obtained to approximate the temperature of the surface of the telescope tube (at 2-D level) through the following expression:

$$T_i(x,z,t)=\sum_{l=1}^{n}W_l(x,z)T_l(t) \qquad (3)$$

where $T_l(t)$ *denotes the measured value at the* l_{th} node of the element; and W_l (x,z) denotes the interpolation weighing function.

The resulting tube temperature gradients were obtained along the r and z coordinates computed as follows:

$$\frac{\partial T_i}{\partial z}=\sum_{l=1}^{n}T_l\frac{\partial w_l}{\partial z} \qquad (4) \qquad \text{and} \qquad \frac{\partial T_i}{\partial x}=\sum_{l=1}^{n}T_l\frac{\partial w_l}{\partial x} \qquad (5)$$

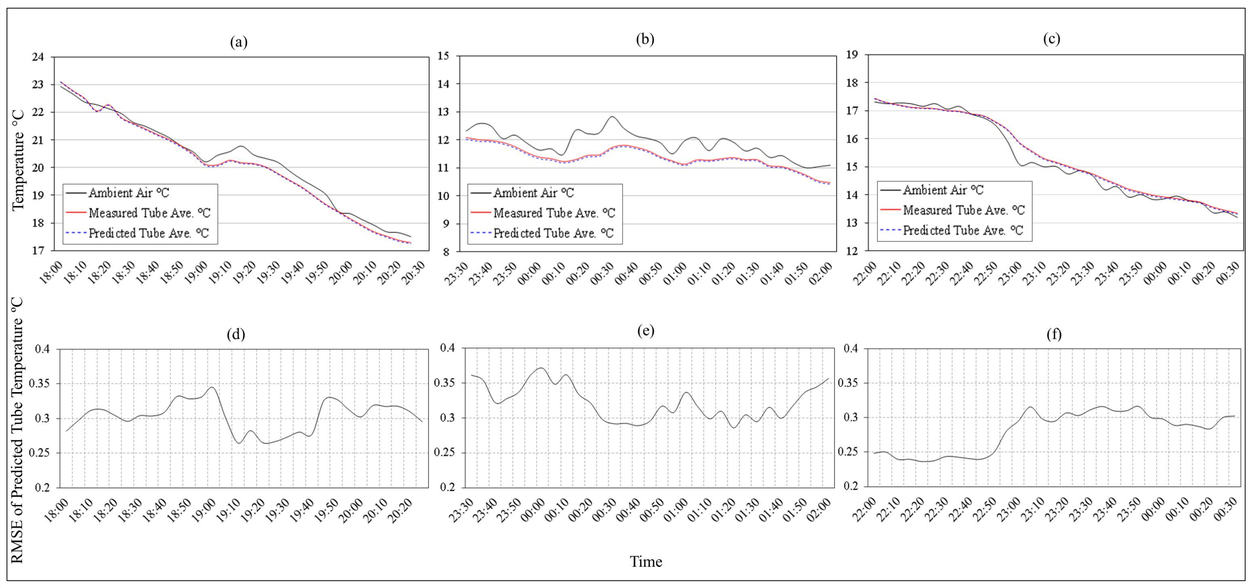

Figure 2. Temperature profiles of ambient air, the measured and predicted tube-surface temperature on the evening of the 24th (a), 25th (b) and 26th (c) September 2016. The predicted tube temperature in the respective days is accompanied by the corresponding RMSE graphs shown in (d), (e) and (f) which indicates the accuracy of the predicted temperatures at unmeasured locations around the tube i.e. error between

4. Results and Conclusion

4.1. Measured and predicted temperatures of the tube surface

Results shown in Figure 2 (a, b and c) indicate a timely response of the tube temperature (measured and predicted) with respect to the varying ambient air temperature during the night at different time periods. In particular, the profile of the predicted tube temperature at unmeasured locations virtually overlaps with the profile of measured tube temperature. This means, the overall tube structure (primarily due to its thermodynamic materials properties) thermally behaves like an isotherm during nighttime to early morning hours, with max-min measured tube temperature variations reaching approximately 1.62 °C (Figure 2 b) coupled with a standard deviation of ± 0.40 °C. The accuracy of the predicted tube temperature is confirmed by the corresponding RMSE plots, which show variation of error in the range 0.26-0.34 °C (d), 0.29-0.37 °C (e) and 0.24-0.32 °C (f). Furthermore, additional results (not visually depicted in Figure 2) gives an improved variation of error in the range 0.19-0.24 °C for predicted tube temperature of 19.48-21.90 °C; this comes from the tube data measured on 9th September 2016 spanning the time from 20:00 to 22:35. In overall, the predicted temperatures approached the targeted accuracy (± 0.3 °C) and may provide a realistic temperature distribution of the LLR tube thermal state.

4.2. Finite element modelling of the tube thermal gradients

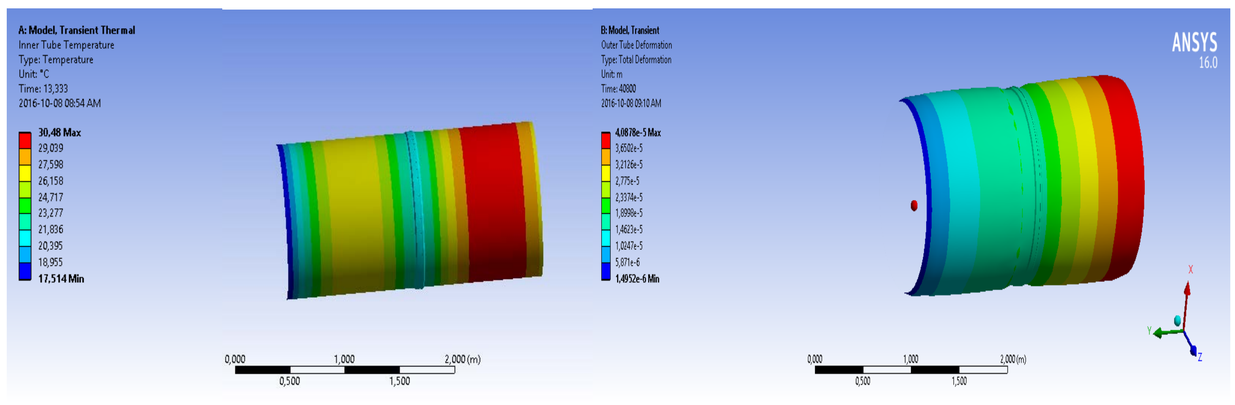

Figure 3. Showing modelled thermal gradients of tube-surface for data that correspond to the samples obtained on the evening of the 24th September (left)) and an the corresponding thermal deformations (right).

The thermal gradients corresponding to the above temperature profiles as described in Figure 2. lie between 0,2 and 0.5 °C. The corresponding thermal gradients have values between 10 .4 mm and 20.8 mm.

4.3. Conclusion

The results obtained from the interpolating weighing function gives values that have an RMS ± 0.3 °C. Given the fact that these results were validated using (reference) sensors mounted onto the same tube surface, the proposed algorithm could predict temperatures that are located very far from measuring nodes.

Acknowledgements

Special thanks to Inkaba ye Afrika, the Department of Science and Technology of South Africa and HartRAO for support. We acknowledge research support in part by the National Research Foundation of South Africa for the grant, Unique Grant No. 93952. Any opinion, finding and conclusion or recommendation expressed in this material is that of the author(s) and the NRF does not accept any liability in this regard.

Selected references

[1] Murphy Jr, T., Adelberger, E.G., Battat, J., Carey, L., Hoyle, C.D., LeBlanc, P., Michelsen, E., Nordtvedt, K., Orin, A. and Strasburg, J.D., 2008. The apache point observatory lunar laser-ranging operation: instrument description and first detections. Publications of the Astronomical Society of the Pacific, 120(863): 20-37.

[2] Combrinck, L., 2014. Development of a high accuracy, user-friendly Lunar Laser Ranging telescope steering and pointing software package at HartRAO, Poster (No. 3004) presented at the 19th International workshop on laser ranging.

[3] Tsela, P., Combrinck, W., Botha, R. and Ngcobo, B., 2016. A proposed mathematical model of thermal variations on the HartRAO Lunar Laser Ranging telescope for enhanced test of Earth-Moon system dynamics. South African Journal of Geology, 119(1): 83-90.

[4] Reddy, J.N. and Gartling, D.K., 2010. The finite element method in heat transfer and fluid dynamics. CRC press.